

## Performance enhancement of perovskite solar cells with Mg-doped TiO<sub>2</sub> compact film as the hole-blocking layer

Jing Wang, Minchao Qin, Hong Tao, Weijun Ke, Zhao Chen, Jiawei Wan, Pingli Qin, Liangbin Xiong, Hongwei Lei, Huaqing Yu, and Guojia Fang

Citation: *Applied Physics Letters* **106**, 121104 (2015); doi: 10.1063/1.4916345

View online: <http://dx.doi.org/10.1063/1.4916345>

View Table of Contents: <http://scitation.aip.org/content/aip/journal/apl/106/12?ver=pdfcov>

Published by the [AIP Publishing](#)

---

### Articles you may be interested in

Double functions of porous TiO<sub>2</sub> electrodes on CH<sub>3</sub>NH<sub>3</sub>PbI<sub>3</sub> perovskite solar cells: Enhancement of perovskite crystal transformation and prohibition of short circuiting  
*APL Mat.* **2**, 081511 (2014); 10.1063/1.4891597

MgO-hybridized TiO<sub>2</sub> interfacial layers assisting efficiency enhancement of solid-state dye-sensitized solar cells  
*Appl. Phys. Lett.* **104**, 063303 (2014); 10.1063/1.4864319

Hydrogenated TiO<sub>2</sub> film for enhancing photovoltaic properties of solar cells and self-sensitized effect  
*J. Appl. Phys.* **114**, 213505 (2013); 10.1063/1.4832783

Performance improvement of inverted polymer solar cells by doping Au nanoparticles into TiO<sub>2</sub> cathode buffer layer  
*Appl. Phys. Lett.* **103**, 233303 (2013); 10.1063/1.4840319

Carrier recombination losses in inverted polymer: Fullerene solar cells with ZnO hole-blocking layer from transient photovoltage and impedance spectroscopy techniques  
*J. Appl. Phys.* **109**, 074514 (2011); 10.1063/1.3561437

---

The advertisement features a photograph of the Model PS-100 cryogenic probe station, which is a complex piece of scientific equipment with various mechanical components and a probe. The background is a gradient of blue. The text is arranged around the image: 'Model PS-100 Tabletop Cryogenic Probe Station' on the left, the 'Lake Shore CRYOTRONICS' logo in the center-right, and the slogan 'An affordable solution for a wide range of research' at the bottom right.

**Model PS-100**  
Tabletop Cryogenic  
Probe Station

**Lake Shore**  
CRYOTRONICS

*An affordable solution for  
a wide range of research*

## Performance enhancement of perovskite solar cells with Mg-doped TiO<sub>2</sub> compact film as the hole-blocking layer

Jing Wang,<sup>1</sup> Minchao Qin,<sup>1</sup> Hong Tao,<sup>1</sup> Weijun Ke,<sup>1</sup> Zhao Chen,<sup>1</sup> Jiawei Wan,<sup>1</sup> Pingli Qin,<sup>1</sup> Liangbin Xiong,<sup>1,2</sup> Hongwei Lei,<sup>1</sup> Huaqing Yu,<sup>2</sup> and Guojia Fang<sup>1,a)</sup>

<sup>1</sup>Key Lab of Artificial Micro- and Nano-Structures of Ministry of Education of China, Department of Electronic Science and Technology, School of Physics and Technology, Wuhan University, Wuhan 430072, People's Republic of China

<sup>2</sup>School of Physics and Electronic-Information Engineering, Hubei Engineering University, Xiaogan 432000, People's Republic of China

(Received 20 January 2015; accepted 16 March 2015; published online 23 March 2015)

In this letter, we report perovskite solar cells with thin dense Mg-doped TiO<sub>2</sub> as hole-blocking layers (HBLs), which outperform cells using TiO<sub>2</sub> HBLs in several ways: higher open-circuit voltage ( $V_{oc}$ ) (1.08 V), power conversion efficiency (12.28%), short-circuit current, and fill factor. These properties improvements are attributed to the better properties of Mg-modulated TiO<sub>2</sub> as compared to TiO<sub>2</sub> such as better optical transmission properties, upshifted conduction band minimum (CBM) and downshifted valence band maximum (VBM), better hole-blocking effect, and higher electron life time. The higher-lying CBM due to the modulation with wider band gap MgO and the formation of magnesium oxide and magnesium hydroxides together resulted in an increment of  $V_{oc}$ . In addition, the Mg-modulated TiO<sub>2</sub> with lower VBM played a better role in the hole-blocking. The HBL with modulated band position provided better electron transport and hole blocking effects within the device. © 2015 AIP Publishing LLC.

[<http://dx.doi.org/10.1063/1.4916345>]

Organolead halide perovskites (CH<sub>3</sub>NH<sub>3</sub>PbX<sub>3</sub>, X = I, Br, and Cl) as light absorbers for solar cells received widespread attention, due to their optimal band gap, large absorption coefficient, and high charge mobilities.<sup>1–6</sup> When irradiated with photoenergy over the bandgap, electron-hole pairs are generated in CH<sub>3</sub>NH<sub>3</sub>PbX<sub>3</sub> and subsequently the electrons inject into the electron transport layer (ETL), while the holes inject into the hole transport layer (HTL).<sup>7</sup> These electrons and holes give a photovoltage, which is highly related with the difference between the conduction band minimum (CBM) in ETL and the valence band maximum (VBM) in HTL. Here, the ETL is referred to as a mesoporous layer and a compact layer (such as TiO<sub>2</sub> (Ref. 8) and ZnO<sup>9</sup>). The compact layer was commonly named as hole-blocking layer (HBL) because it could avoid the heavy recombination of the holes which were generated in the CH<sub>3</sub>NH<sub>3</sub>PbX<sub>3</sub> and the electrons, which were existed in both CH<sub>3</sub>NH<sub>3</sub>PbX<sub>3</sub> and the HTL at the surface of the fluorine-doped tin oxide (FTO).<sup>10–13</sup>

Doping or mixing TiO<sub>2</sub> with other elements is widely conducted to tailor the properties of photoanode in dye sensitized solar cells (DSSCs).<sup>14–18</sup> Doping TiO<sub>2</sub> compact film with metal elements has also been used in DSSCs. As reported, Nb-doped TiO<sub>2</sub> compact film suppressed the charge recombination from FTO to electrolyte, reducing the interfacial resistance between TiO<sub>2</sub> and FTO.<sup>19</sup> Li-doped TiO<sub>2</sub> compact layer facilitated the electron transfer from nano-TiO<sub>2</sub> to transparent conductive oxide surface due to the reduced interfacial resistance between the two layers.<sup>20</sup> Researches of doping in the compact layer of the perovskite solar cells have also been done. Wang *et al.*<sup>21</sup> reported graphene nanoflakes

modified TiO<sub>2</sub> HBL provided superior charge-collection in the nanocomposites and improved the photovoltaic performance. Zhou *et al.*<sup>22</sup> used yttrium-doped TiO<sub>2</sub> compact layer for better transferring electrons while blocking holes. Mg-doped TiO<sub>2</sub> nanorods were used as the ETL for perovskite solar cells, resulting in a marked increase of open-circuit voltage ( $V_{oc}$ ). Unfortunately, Mg-doping caused a decline in the short current density ( $J_{sc}$ ) performance because of the upshifted CBM.<sup>23</sup>

To overcome this adversity, we introduce Mg into the compact TiO<sub>2</sub> HBL of the perovskite solar cells, which can both provide better hole-blocking effect and be still convenient for electron transfer from perovskite to TiO<sub>2</sub>. Our comparative studies reveal that perovskite solar cells using Mg-doped TiO<sub>2</sub> HBLs outperform the controlled cells using TiO<sub>2</sub> HBLs due to the following reasons: (1) Mg-doped TiO<sub>2</sub> has a higher CBM and lower VBM that match better with the energy bands of the porous TiO<sub>2</sub> and CH<sub>3</sub>NH<sub>3</sub>PbI<sub>3</sub>, resulting in cells with higher values of  $V_{oc}$  and fill factor (FF); (2) Mg-doped TiO<sub>2</sub> has a wider band gap and better optical transmission properties, leading to cells with greater values of  $J_{sc}$ ; and (3) Mg-doped TiO<sub>2</sub> exhibits a much longer electron life time and a smaller contact resistance, indicating a reduced recombination of electrons and holes which makes an improvement of both the  $V_{oc}$  and the  $J_{sc}$ . We obtained an optimized Mg-doped TiO<sub>2</sub> based device with a 100 mV enhancement in  $V_{oc}$  than that of the pure TiO<sub>2</sub> based device together with improvement in the  $J_{sc}$  and the FF.

The perovskite solar cells were fabricated on FTO glass substrates (about 14  $\Omega$  sq<sup>-1</sup>). Before fabrication, the substrates were rinsed by the same way we used before.<sup>24</sup> The Mg-doped TiO<sub>2</sub> compact layer was prepared by spin coating. Different amount of magnesium acetate tetrahydrate was

<sup>a)</sup> Author to whom correspondence should be addressed. Electronic mail: gjfang@whu.edu.cn

added in 0.05M ethanol solution of  $\text{TiCl}_4$ . The above-mentioned solution was spin-coated on the FTO glass at 2000 r.p.m. for 30 s and sintered at  $500^\circ\text{C}$  for 15 min. A 200 nm  $\text{TiO}_2$  porous layer, an organic-inorganic perovskite  $\text{CH}_3\text{NH}_3\text{PbI}_3$  layer, and a layer of hole transport material (HTM) were prepared by the same way we used before.<sup>25,26</sup> A thin layer of gold electrode was finally deposited by thermal evaporation.

The morphology and components of Mg-doped  $\text{TiO}_2$  compact films were observed by a high-resolution field emission scanning electron microscope (SEM, JSM 6700F) and energy dispersive X-ray spectrometry (EDX). X-ray photoelectron spectroscopy (XPS) and ultraviolet photoelectron spectroscopy (UPS) were recorded on a XPS/UPS system (Thermo Scientific, ESCLAB 250Xi, USA). Transmission spectra of the HBLs were measured by an UV-Vis-NIR spectrophotometer (CARY5000, Varian). The photovoltaic characteristics were recorded by a standard ABET Sun 2000 Solar Simulator under  $100\text{ mW cm}^{-2}$ , AM 1.5 simulated irradiation. Photocurrent density-voltage ( $J$ - $V$ ) characteristics were collected using a CHI660D electrochemical workstation (Shanghai, China). The scan rate was  $10\text{ mV s}^{-1}$ . The active area of all devices was  $0.09\text{ cm}^2$ .

Fig. 1(a) is the sketch of the Mg-doped  $\text{TiO}_2$  HBL perovskite solar cells. After irradiated with photoenergy over the bandgap of perovskite (i.e.,  $\text{CH}_3\text{NH}_3\text{PbI}_3$ ), electrons and holes are generated and subsequently injected into  $\text{TiO}_2$  electron transport material and spiro-OMeTAD HTM, respectively. The compact layer acts as an important role to reduce the recombination of electrons and holes and transport electrons as well. Fig. 1(b) shows the  $J$ - $V$  characteristics of non-doped and Mg-doped  $\text{TiO}_2$  compact layer perovskite solar

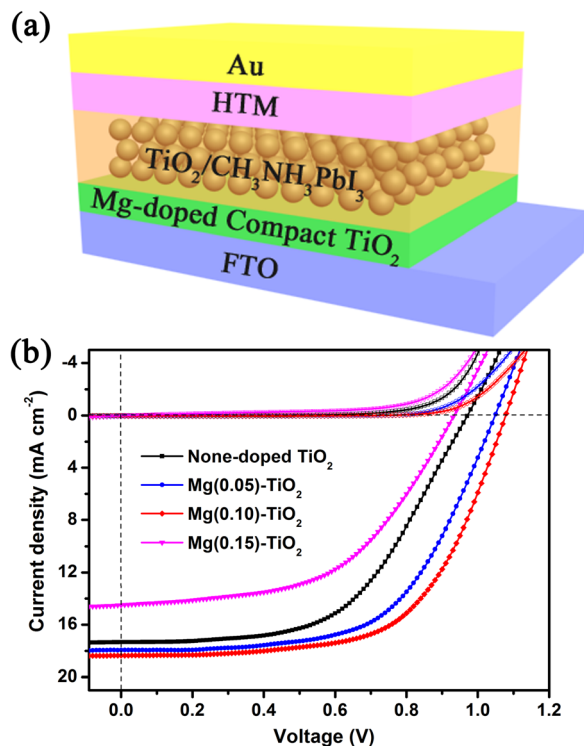


FIG. 1. (a) The sketch of the Mg-doped  $\text{TiO}_2$  HBL perovskite solar cells. (b)  $J$ - $V$  curves of the perovskite solar cells with the non-doped and Mg-doped  $\text{TiO}_2$  compact layers.

TABLE I. Photovoltaic parameters (average values) for the perovskite solar cells with different amount of Mg doping.

	$V_{oc}$ (V)	$J_{sc}$ ( $\text{mA/cm}^2$ )	FF (%)	PCE (%)
None-doped $\text{TiO}_2$	$0.98 \pm 0.02$	$17.31 \pm 0.53$	$0.54 \pm 0.01$	$9.16 \pm 0.65$
Mg(0.05)- $\text{TiO}_2$	$1.05 \pm 0.01$	$17.94 \pm 0.25$	$0.59 \pm 0.01$	$11.11 \pm 0.46$
Mg(0.10)- $\text{TiO}_2$	$1.08 \pm 0.01$	$18.34 \pm 0.31$	$0.62 \pm 0.01$	$12.28 \pm 0.53$
Mg(0.15)- $\text{TiO}_2$	$0.93 \pm 0.02$	$14.51 \pm 0.33$	$0.52 \pm 0.02$	$7.02 \pm 0.59$

cells. And the photovoltaic characteristics are summarized in Table I. We name the films at an increasing Mg-Ti molar ratio of 0, 0.05, 0.10, and 0.15 as none-doped  $\text{TiO}_2$ , Mg(0.05)- $\text{TiO}_2$ , Mg(0.10)- $\text{TiO}_2$ , and Mg(0.15)- $\text{TiO}_2$  films, respectively. The none-doped  $\text{TiO}_2$  cell showed a moderate performance (a  $V_{oc}$  of 0.98 V, and a power conversion efficiency (PCE) of 9.16%). After adding 5 and 10 at. % Mg into the blocking layer, the  $V_{oc}$  increased to 1.05 V and 1.08 V, respectively. Besides, there were also enhancements in the  $J_{sc}$  and the FF as expected. Nevertheless, all the parameters declined when the amount of Mg was added up to 15 at. %. The  $V_{oc}$  of the Mg(0.15)- $\text{TiO}_2$  cell was down to 0.93 V and the cell exhibited poor performance. This result also corresponds to the dark current densities, which can be drawn from the dark  $J$ - $V$  curves, indicating the Mg(0.10)- $\text{TiO}_2$  cell has the lowest recombination. The series resistance ( $R_s$ ) derived from the  $J$ - $V$  curves has an impact on the FF.<sup>27</sup> The  $R_s$  of the none-doped  $\text{TiO}_2$ , Mg(0.05)- $\text{TiO}_2$ , Mg(0.10)- $\text{TiO}_2$ , and Mg(0.15)- $\text{TiO}_2$  perovskite solar cells are 20.10  $\Omega$ , 14.55  $\Omega$ , 12.51  $\Omega$ , and 21.47  $\Omega$ , respectively. So the FF of the cells shows a downward trend after rising first after Mg-doping. Hysteresis effect in the  $J$ - $V$  curves can be observed in the supplementary material.<sup>34</sup> We have also added magnesium acetate tetrahydrate into the widely used compact  $\text{TiO}_2$  solution,<sup>28</sup> whose major material was tetrabutyl titanate in ethanol solution. However, after adding very small proportion of magnesium acetate tetrahydrate, the tetrabutyl titanate would hydrolyze immediately, making the compact film full of pores and agglomerated particles. So  $\text{TiCl}_4$  which hydrolyzed less was used in our study.

To illustrate the mechanism of the enhanced performance of the Mg-doped  $\text{TiO}_2$  perovskite solar cells, a series of characterizations have been done. The SEM-EDX spectrum for Mg(0.10)- $\text{TiO}_2$  (see Fig. S2 in the supplementary material<sup>34</sup>) demonstrated the existence of magnesium in the  $\text{TiO}_2$  film after sintering. X-ray diffraction was measured to study the structure of the films (see the supplementary material<sup>34</sup>). The existence of  $\text{MgTiO}_3$  in the Mg(0.10)- $\text{TiO}_2$  film shown in the XRD patterns indicated Mg(II) substituted crystal lattice in anatase  $\text{TiO}_2$ , which may result in a higher-lying CBM of the compact layer. Surface images of the doped and non-doped  $\text{TiO}_2$  compact film were observed by SEM (see Fig. S4 in the supplementary material<sup>34</sup>). The films that the amount of Mg-doping is no more than 10 at. % are very alike, which are dense and even. However, the film quality deteriorates because of the appearance of larger particles after the doping amount rises to 15 at. %. It is probably because the crystal water in magnesium acetate tetrahydrate accelerates the hydrolyzation of titanium tetrachloride in the mixture solution, thus, forming large particles of  $\text{TiO}_2$ . So

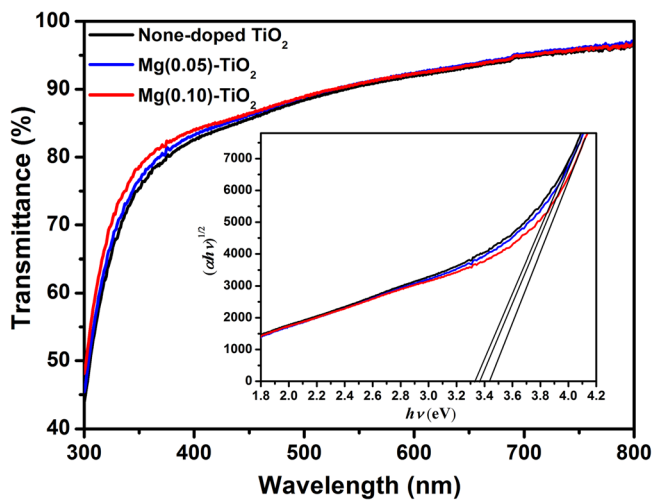


FIG. 2. Transmission spectra of the none-doped  $\text{TiO}_2$ , the  $\text{Mg}(0.05)\text{-TiO}_2$ , and the  $\text{Mg}(0.10)\text{-TiO}_2$  films. The inset shows the Tauc plot of the films.

the  $\text{Mg}(0.15)\text{-TiO}_2$  film is not qualified to be the HBL of a perovskite solar cell and we did not focus on the characteristics of  $\text{Mg}(0.15)\text{-TiO}_2$  film.

The transmission spectra of non-doped and Mg-doped  $\text{TiO}_2$  compact films are shown in Fig. 2. The optical absorption edges of the Mg-doped  $\text{TiO}_2$  films shift to shorter wavelength range and better transmission is gained, especially at short wavelength region. Better transmission contributed to the improved  $J_{sc}$ . The blue-shift of the light absorption is in consequence of the wider energy band gap. The optical band gaps derived from Tauc plot  $((\alpha h\nu)^{1/2}$  vs. eV), as shown in the inset of Fig. 2, demonstrate the band gaps of non-doped  $\text{TiO}_2$ ,  $\text{Mg}(0.05)\text{-TiO}_2$ , and  $\text{Mg}(0.10)\text{-TiO}_2$  are 3.33 eV, 3.36 eV, and 3.44 eV, respectively. Here,  $\alpha = -(\ln T/t)$ , where  $T$  is the transmission of the film and  $t$  is the thickness of the film.

UPS characterization of none-doped  $\text{TiO}_2$  and  $\text{Mg}(0.10)\text{-TiO}_2$  was done to get the relative accurate position of the energy band, and the result is shown in Fig. 3(a). The full UPS spectra using He I radiation are located in the middle position. Work function (WF) is derived from subtracting the cut-off banding energy (the left spectra of Fig. 3(a)) with the photon energy (21.22 eV). It is known that the WF of  $\text{MgO}^{29}$  was less than that of  $\text{TiO}_2$ , so the WF shifted up a little after the Mg-doping. None-doped  $\text{TiO}_2$  showed a WF of 5.33 eV and  $\text{Mg}(0.10)\text{-TiO}_2$  showed a WF of 5.29 eV. The expanded valence spectra are shown in the right of Fig. 3(a). The peaks of the none-doped  $\text{TiO}_2$  film and the  $\text{Mg}(0.10)\text{-TiO}_2$  film, respectively, center at 2.17 eV and 2.29 eV. The peak values are the distance between the VBM and the WF. So the VBM position of the none-doped  $\text{TiO}_2$  and the  $\text{Mg}(0.10)\text{-TiO}_2$  are 7.51 eV and 7.58 eV, respectively. From the known data, the energy level diagram of perovskite solar cells with none-doped  $\text{TiO}_2$  compact layer and  $\text{Mg}(0.10)\text{-TiO}_2$  compact layer is shown in Fig. 3(b). Doping Mg into  $\text{TiO}_2$  makes the energy band broadening, moving the bottom of the conduction band up and shifting the top of the valence band down. The elevated CBM contributes to the increase of the  $V_{oc}$ . The upshifted CBM of the blocking layer is more compatible with the mesoporous  $\text{TiO}_2$  and the  $\text{CH}_3\text{NH}_3\text{bPI}_3$ ,

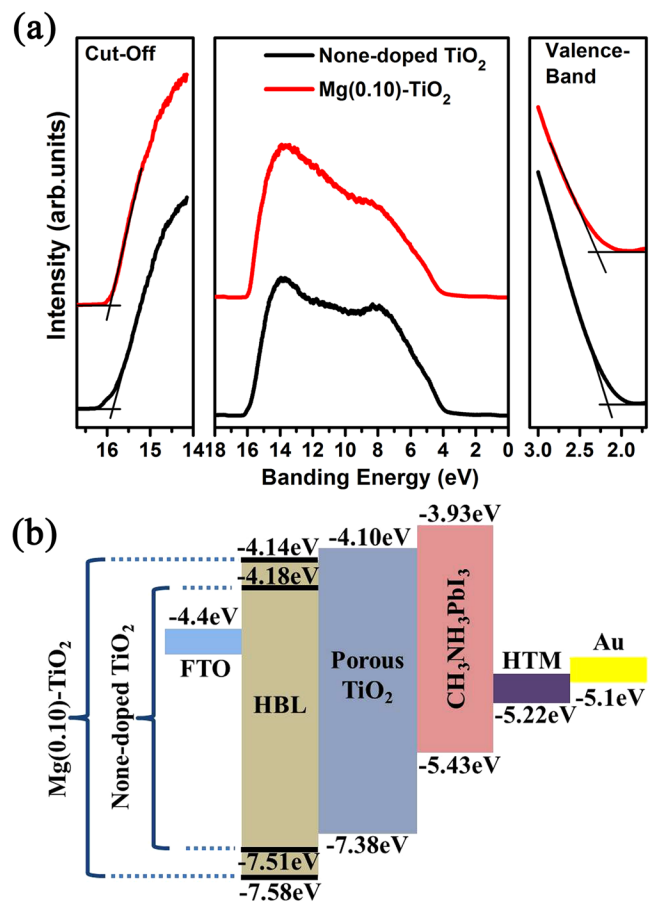


FIG. 3. (a) UPS spectra of none-doped  $\text{TiO}_2$  and  $\text{Mg}(0.10)\text{-TiO}_2$  films. The full UPS spectra (center), secondary-electron cut-off (left), and the valence-band region (right) are included. (b) Energy level diagram of perovskite solar cells with none-doped  $\text{TiO}_2$  and  $\text{Mg}(0.10)\text{-TiO}_2$  HBLs.

reducing the energy loss though the electron transportation. The electron quasi-Fermi level also moves up because of the upshifted CBM. XPS<sup>30</sup> spectra (see Fig. S5 in the supplementary material<sup>34</sup>) of the  $\text{Mg}(0.10)\text{-TiO}_2$  film show that there is adsorption of  $\text{OH}^-$  groups except Mg-O bonding. According to the XPS spectra and the literature report,<sup>23</sup> there should be a good thin insulating layer of magnesium oxide and magnesium hydroxides on the  $\text{TiO}_2$  surface due to the similarity of the ionic radii of  $\text{Mg}^{2+}$  (0.066 nm) and  $\text{Ti}^{4+}$  (0.061 nm), which surpasses the recombination and shows better hole-blocking effect, achieving a further improvement of  $V_{oc}$ . The lower VBM of Mg-doped  $\text{TiO}_2$  compact layer could benefit the  $J_{sc}$  and the FF. The downshifted VBM could be more effective to block holes, resulting in less recombination of electrons and holes at the film surface and thus, giving a better  $J_{sc}$  and FF. Besides, in this work, Mg was doped in the very thin dense  $\text{TiO}_2$  layer, whose upshifted CBM was not higher than that of porous  $\text{TiO}_2$ , so the electron transfer was efficient between the  $\text{CH}_3\text{NH}_3\text{PbI}_3$  and two layers of  $\text{TiO}_2$ . As a result, the ETL in our cell was effective and the decrease of  $J_{sc}$  did not occur.

To further verify the performance enhancement of the Mg-doped  $\text{TiO}_2$  device, incident photon to current efficiency (IPCE) and open-circuit photovoltage decay (OCVD) were measured. The IPCE spectra are shown in Fig. 4(a). The result is in conformity with the changing

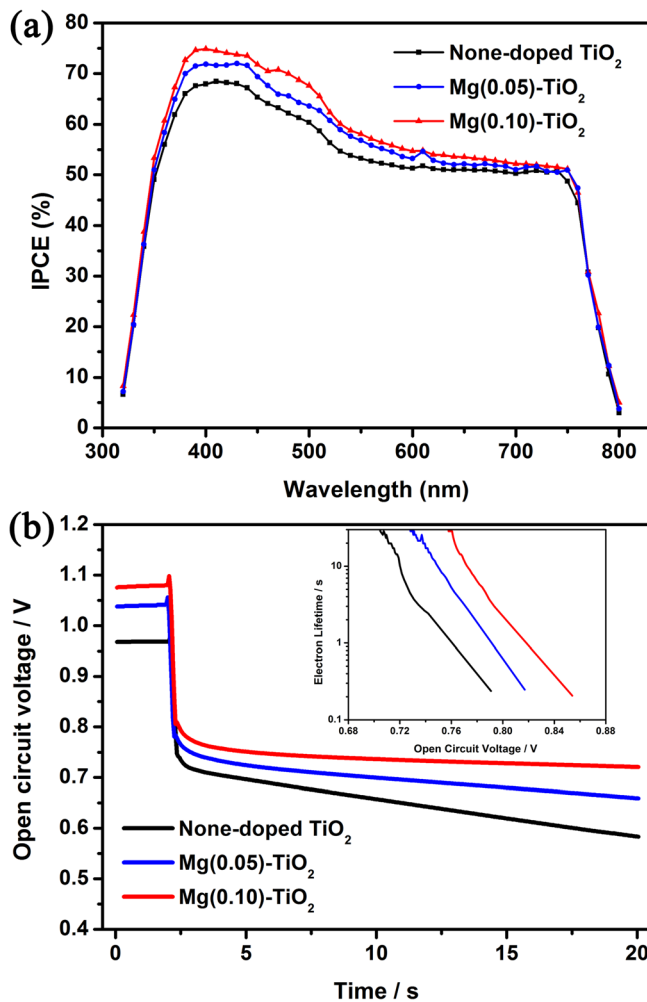


FIG. 4. (a) IPCE spectra and (b) OCVD curves of the perovskite solar cells with the none-doped  $\text{TiO}_2$ , the  $\text{Mg}(0.05)\text{-TiO}_2$ , and the  $\text{Mg}(0.10)\text{-TiO}_2$  compact layers. The inset of (b) is the electron lifetime as a function of  $V_{oc}$  of the solar cells.

trend of  $J_{sc}$  of the perovskite solar cells with different amount of Mg-doping in  $\text{TiO}_2$  blocking layer. Mg-doping mainly benefits the IPCE at the short wavelength region, which should be due to the better light transmission in the corresponding wavelength range and due to the better charge transportation of the cell.

The OCVD<sup>31–33</sup> was measured to understand the effect of different HBLs on the electron lifetime. In this measurement, the decay of photovoltage after making the device under dark condition was recorded. Fig. 4(b) illustrates the voltage decay curves of the perovskite solar cells with the non-doped  $\text{TiO}_2$  layer, the  $\text{Mg}(0.05)\text{-TiO}_2$  layer, and the  $\text{Mg}(0.10)\text{-TiO}_2$  layer. It can be seen that there are three voltage dependent regions: (1) the high voltage region under illumination, related to free electrons; (2) the exponential increase region when the light was just lost, reflecting internal trapping and detrapping of the semiconductor particles; and (3) the inverted parabola region at relative low photovoltage due to the effect of surface states.<sup>31</sup> What we concerned about is the exponential increase region which reveals the electron-hole recombination process.<sup>24</sup>

The electron lifetimes under open-circuit conditions can be calculated from the decay curves by formula (1)

$$\tau_n = -\frac{k_B T}{e} \left( \frac{dV_{oc}}{dt} \right)^{-1}, \quad (1)$$

where  $k_B$  is the Boltzmann constant,  $T$  is the temperature, and  $e$  is the positive elementary charge. And the electron lifetime as the function of the  $V_{oc}$  is shown in the inset of Fig. 4(b). As a result, the electron lifetimes of the Mg-doped  $\text{TiO}_2$  samples are longer than that of the none-doped  $\text{TiO}_2$  sample. For example, when the voltage is 0.78 V, the electron lifetimes are 0.40 s, 1.82 s, and 6.25 s for the solar cells with the none-doped  $\text{TiO}_2$ , the  $\text{Mg}(0.05)\text{-TiO}_2$ , and the  $\text{Mg}(0.10)\text{-TiO}_2$  HBLs, respectively. As expected,  $\text{TiO}_2$  HBL with Mg-doping is beneficial to the electron transportation as the electron lifetimes become longer. In other word, the recombination of electrons and holes is suppressed because of Mg doping, which is an important reason for the improved photovoltaic properties.

In summary, we have developed the perovskite solar cells with different amount of Mg-doping in  $\text{TiO}_2$  blocking layer. Adding Mg into the blocking layer elevated the position of the CBM of  $\text{TiO}_2$ , which made a contribution to the improvement of the  $V_{oc}$ . Besides, there was also a thin layer of magnesium oxide and magnesium hydroxide formed at the surface of the HBL, which could suppress the recombination at the compact  $\text{TiO}_2$  surface, achieving a further improvement of  $V_{oc}$ . More advantageously, the higher-lying position of the CBM would not hinder the electron transfer between the perovskite and the two  $\text{TiO}_2$  layer, thus, high  $J_{sc}$  and FF were obtained. Furthermore, less recombination and better transmittance also resulted in better  $J_{sc}$  and FF. This work provides a direction for future improvement of perovskite solar cells.

This work was financially supported by the National High Technology Research and Development Program (No. 2015AA050601), the National Basic Research Program (No. 2011CB933300) of China, the National Natural Science Foundation of China (Nos. 61376013, 91433203, and J1210061), the Natural Science Foundation of Jiangsu Province (BK20131186), Suzhou Science and Technology Bureau (SYG201449). We thank the nano center of Wuhan University for SEM, XPS, and UPS measurements.

<sup>1</sup>H. S. Kim, C. R. Lee, J. H. Im, K. B. Lee, T. Moehl, A. Marchioro, S. J. Moon, R. Humphry-Baker, J. H. Yum, J. E. Moser, M. Grätzel, and N. G. Park, *Sci. Rep.* **2**, 591 (2012).

<sup>2</sup>J. M. Ball, M. M. Lee, A. Hey, and H. J. Snaith, *Energy Environ. Sci.* **6**, 1739 (2013).

<sup>3</sup>D. Liu and T. L. Kelly, *Nat. Photonics* **8**, 133 (2014).

<sup>4</sup>Z. Ku, Y. Rong, M. Xu, T. Liu, and H. Han, *Sci. Rep.* **3**, 3132 (2013).

<sup>5</sup>J. Shi, J. Dong, S. Lv, Y. Xu, L. Zhu, J. Xiao, X. Xu, H. Wu, D. Li, and Y. Luo, *Appl. Phys. Lett.* **104**, 063901 (2014).

<sup>6</sup>J. Burschka, N. Pellet, S. J. Moon, R. Humphry-Baker, P. Gao, M. K. Nazeeruddin, and M. Grätzel, *Nature* **499**, 316 (2013).

<sup>7</sup>Q. Lin, A. Armin, R. C. R. Nagiri, P. L. Burn, and P. Meredith, *Nat. Photonics* **9**, 106 (2014).

<sup>8</sup>S. Aharon, S. Gamliel, B. El Cohen, and L. Etgar, *Phys. Chem. Chem. Phys.* **16**, 10512 (2014).

<sup>9</sup>M. H. Kumar, N. Yantara, S. Dharani, M. Grätzel, S. Mhaisalkar, P. P. Boix, and N. Mathews, *Chem. Commun.* **49**, 11089 (2013).

<sup>10</sup>N. G. Park, *J. Phys. Chem. Lett.* **4**, 2423 (2013).

<sup>11</sup>B. Conings, L. Baeten, C. De Dobbelaere, J. D'Haen, J. Manca, and H. G. Boyen, *Adv. Mater.* **26**, 2041 (2014).

- <sup>12</sup>M. M. Lee, J. Teuscher, T. Miyasaka, T. N. Murakami, and H. J. Snaith, *Science* **338**, 643 (2012).
- <sup>13</sup>Y. Wu, X. Yang, H. Chen, K. Zhang, C. Qin, J. Liu, W. Peng, A. Islam, E. Bi, and F. Ye, *Appl. Phys. Express* **7**, 052301 (2014).
- <sup>14</sup>T. Chen, W. Hu, J. Song, G. H. Guai, and C. M. Li, *Adv. Funct. Mater.* **22**, 5245 (2012).
- <sup>15</sup>S. Iwamoto, Y. Sazanami, M. Inoue, T. Inoue, T. Hoshi, K. Shigaki, M. Kaneko, and A. Maenosono, *ChemSusChem* **1**, 401 (2008).
- <sup>16</sup>J. Zhang, W. Peng, Z. Chen, H. Chen, and L. Han, *J. Phys. Chem. C* **116**, 19182 (2012).
- <sup>17</sup>K. Kakiage, T. Tokutome, S. Iwamoto, T. Kyomen, and M. Hanaya, *Chem. Commun.* **49**, 179 (2013).
- <sup>18</sup>S. Yang, H. Kou, S. Song, H. Wang, and W. Fu, *Colloids Surf., A* **340**, 182 (2009).
- <sup>19</sup>S. Lee, J. H. Noh, H. S. Han, D. K. Yim, D. H. Kim, J. K. Lee, J. Y. Kim, H. S. Jung, and K. S. Hong, *J. Phys. Chem. C* **113**, 6878 (2009).
- <sup>20</sup>W. Q. Zhou, Y. M. Lu, C. Z. Chen, Z. Y. Liu, and C. B. Cai, *J. Inorg. Mater.* **26**, 819 (2011).
- <sup>21</sup>J. T. W. Wang, J. M. Ball, E. M. Barea, A. Abate, J. A. Alexander-Webber, J. Huang, M. Saliba, I. N. Mora-Sero, J. Bisquert, and H. J. Snaith, *Nano Lett.* **14**, 724 (2014).
- <sup>22</sup>H. Zhou, Q. Chen, G. Li, S. Luo, T. B. Song, H. S. Duan, Z. Hong, J. You, Y. Liu, and Y. Yang, *Science* **345**, 542 (2014).
- <sup>23</sup>K. Manseki, T. Ikeya, A. Tamura, T. Ban, T. Sugiura, and T. Yoshida, *RSC Adv.* **4**, 9652 (2014).
- <sup>24</sup>H. Tao, G. Fang, W. Ke, W. Zeng, and J. Wang, *J. Power Sources* **245**, 59 (2014).
- <sup>25</sup>X. Hu, J. Xiong, Y. Tang, C. Zhou, and J. Yang, *Phys. Status Solidi A* **212**, 585 (2015).
- <sup>26</sup>W. Ke, G. Fang, J. Wang, P. Qin, H. Tao, H. Lei, Q. Liu, X. Dai, and X. Zhao, *ACS Appl. Mater. Interfaces* **6**, 15959 (2014).
- <sup>27</sup>J. H. Heo, S. H. Im, J. H. Noh, T. N. Mandal, C. S. Lim, J. A. Chang, Y. H. Lee, H. J. Kim, A. Sarkar, and M. K. Nazeeruddin, *Nat. Photonics* **7**, 486 (2013).
- <sup>28</sup>W. Zeng, G. Fang, X. Wang, Q. Zheng, B. Li, H. Huang, H. Tao, N. Liu, W. Xie, and X. Zhao, *J. Power Sources* **229**, 102 (2013).
- <sup>29</sup>A. Kolmakov, J. Stultz, and D. Goodman, *J. Chem. Phys.* **113**, 7564 (2000).
- <sup>30</sup>Y. Zhang, W. J. Jiang, X. Zhang, L. Guo, J. S. Hu, Z. Wei, and L. J. Wan, *Phys. Chem. Chem. Phys.* **16**, 13605 (2014).
- <sup>31</sup>J. Bisquert, A. Zaban, M. Greenshtein, and I. Mora-Seró, *J. Am. Chem. Soc.* **126**, 13550 (2004).
- <sup>32</sup>A. Zaban, M. Greenshtein, and J. Bisquert, *ChemPhysChem* **4**, 859 (2003).
- <sup>33</sup>X. Sun, Y. Liu, Q. Tai, B. Chen, T. Peng, N. Huang, S. Xu, T. Peng, and X. Zhao, *J. Phys. Chem. C* **116**, 11859 (2012).
- <sup>34</sup>See supplementary material at <http://dx.doi.org/10.1063/1.4916345> for the hysteresis effect in the  $J$ - $V$  curves, SEM-EDX spectrum for Mg(0.10)-TiO<sub>2</sub> nanoparticles, XRD patterns for none-doped TiO<sub>2</sub> and Mg(0.10)-TiO<sub>2</sub> nanoparticles, SEM images of the surfaces of none-doped TiO<sub>2</sub>, Mg(0.10)-TiO<sub>2</sub>, and Mg(0.15)-TiO<sub>2</sub> compact films, and XPS spectra of Mg(0.10)-TiO<sub>2</sub> compact film.